A study on ZnO nanoparticles catalyzed ring opening polymerization of L-lactide

ARTICLE *in* JOURNAL OF POLYMER RESEARCH · SEPTEMBER 2014

Impact Factor: 1.92 · DOI: 10.1007/s10965-014-0537-x

3 AUTHORS, INCLUDING:

Anuradha Rathore
Gujarat University
1 PUBLICATION **2** CITATIONS

SEE PROFILE

J Polym Res (2014) 21:537
DOI 10.1007/s10965-014-0537-x

ORIGINAL PAPER

A study on ZnO nanoparticles catalyzed ring opening polymerization of L-lactide

Harjinder Kaur · Anuradha Rathore · Shinu Raju

Received: 24 April 2014 / Accepted: 18 July 2014

Abstract Facile synthesis of multifunctional organic/inorganic materials is gaining importance. Present study deals with single step synthesis of PLLA/ZnO nanocomposite by ZnO nanoparticles catalyzed ring opening polymerization of L-lactide. The PLLA/ZnO nanocomposites with different ZnO concentrations were prepared and characterized by FT-IR, XRD, TEM, SEM, DSC, TGA, GPC, ^{13}C NMR and ^{1}H NMR etc. Uniform dispersion of ZnO nanoparticles of size 2–10 nm was achieved without any surface modification of the nanoparticles. The results showed that the as-synthesized PLLA/ZnO nanocomposites possessed thermal properties different from PLLA/ZnO nanocomposites synthesized by other techniques. The synthesized nanocomposite also showed excellent photochemical properties which were analyzed by studying decomposition of methylene blue dye.

Keywords Poly(L-lactide) · ZnO nanoparticles · In-situ ring opening polymerization · Thermal properties · Methylene blue degradation

Introduction

The biodegradable and biocompatible polymers have gained significant attention from both ecological and biomedical perspectives in the past decade. In general, synthetic polymers produced from petrochemical products have low recovery/reproduction rates and are not easily degraded in the environment. Rapid growth of municipal waste is driving the efforts towards biodegradable/biocompatible polymers that can be used as renewable resources for polymer manufacturing and reduce the waste volume of synthetic polymers. The most important among biodegradable polymers are aliphatic polyesters [1]. These biodegradable polyesters include poly(lactic acid) (PLA), poly(glycolic acid) (PGA), poly(e-caprolactone) (PCL) and poly(3-hydroxy butyrate((PHB) among which, PLA has received the most attention due to its renewable resources[2], biocompatibility, biodegradation, excellent thermal/mechanical properties and superior transparency of the processed materials[3]. Lactic acid, the monomer unit of PLA is obtained by the process of fermentation of corn, potato, sugar beet and sugar cane. PLA is then synthesized either by the condensation polymerization of lactic acid monomer or by ring-opening polymerization of lactide monomer. PLA which is thus produced from renewable resources is a linear aliphatic thermoplastic polyester and is readily biodegradable through hydrolytic and enzymatic pathways. Due to its property of biodegradability, PLA has acquired wide range of biological applications for itself that include surgical implantsb[4], tissue culture[5], resorbable sutures[6], controlled release systems [7, 8]. Mechanical properties of PLA are also comparable to those of thermoplastic polymers and it can be reasonably substituted for conventional polymers in areas such as packaging [9, 10].

Nanoparticles are being employed increasingly to produce nanocomposites, either to enhance mechanical and thermal properties of the biopolymers, or to produce novel materials [11]. A survey of the literature revealed that nanocomposite of PLA and clay [12, 13] have been extensively studied and reviewed. Inclusion of clay (montmorillonite layered silicates) results in increased thermal and barrier properties of PLA. However; addition of clay into PLA could decrease toughness of the polymer. Lately inclusion of metal oxide nanoparticles into polymer matrix has attracted the attention of many workers as they can introduce novel properties to the polymer. PLA blend of TiO_2 has been reported to improve mechanical properties suitable for orthopedic applications [14].

H. Kaur (✉) · A. Rathore · S. Raju
Chemistry Department, School of Sciences, Gujarat University, Ahmedabad, Gujarat, India
e-mail: hk_ss_in@yahoo.com

Published online: 07 August 2014

Nakayama and Hayashi [15] reported increased biodegradability of PLA through photo-degradation when modified TiO_2 nanoparticles were dispersed in PLA. Surface grafted high molecular weight PLA-MgO nanocomposites [16] were reported by Sun et al. To prevent phase separation and aggregation of ZnO nanoparticles, surface modification of nanoparticles with silane was reported by Murariu et al. [17]. A recent report also shows that incorporation of ZnO to PLA enhances mechanical and thermal properties of the composite compared to PLA [18].

Zinc oxide (ZnO) has unique properties and versatile applications in transparent electronics, ultraviolet (UV) light emitters, piezoelectric devices, chemical sensors and spin electronics [19–24]. FDA has approved ZnO as a food additive and it was found that ZnO was neither a skin irritant nor a skin sensitizer. A few articles have reported preparation of PLLA/ZnO by melt-blending process and melt extrusion process [18, 25]. In this study, we propose ZnO nanoparticles as catalyst for ring opening polymerization of L-lactide to synthesize PLLA/ZnO nanocomposite in one step. These nanocomposites have been characterized by various analytical techniques and the effect of ZnO nanoparticle concentration on the thermal properties of PLLA was examined. Further, the effect of PLLA chain on the photocatalytic property of ZnO nanoparticles was analyzed by studying degradation of methylene blue dye.

Experimental part

Materials

All the chemicals used were of analytical grade or of the highest purity available. L-lactide and PLLA standard sample were procured from Aldrich. All the chemicals were used as received. ZnO nanoparticles were synthesized by microwave enhanced solvo-thermal hydrolysis of zinc acetate [26].

Synthesis of PLLA/ZnO nanocomposites

PLLA/ZnO nanocomposites with varying concentration of ZnO were synthesized by ring opening polymerization of L-lactide. In a typical procedure, 20 mg of freshly prepared ZnO nanoparticulates were taken in a round bottom flask of 50 ml along with 20 ml of pure dioxane. A magnetic stirrer was dropped into the flask and the mixture stirred at 60 °C for 1 h to disperse nanoparticles. 2 g of L-lactide was added and then the temperature raised to 80 °C. At this point dioxane was distilled off under vacuum and the flask purged with nitrogen. The flask was completely immersed in oil bath and temperature further raised to 160 °C. The polymerization was allowed to proceed for 5 h. The resulting gel after cooling was dispersed in 10 ml chloroform and then re-precipitated with methanol (five times of chloroform). The white product obtained in quantitative amount was dried in a desiccator overnight.

Characterization

The synthesized compounds were analyzed on Shimadzu FT-IR 8400 spectrophotometer, the sample was mixed with anhydrous fine powder of KBr and the mixture was crushed well. Thin pellets made out of the mixture were then placed into the analytical sample window and the IR spectra were recorded.

X-ray diffraction (XRD) measurements were performed on SEIFERT-FPM by an X-ray diffractometer using Cu Kα radiation source (λ=1.5418) at power 200 kW, approximately 1 g of sample was loaded on the glass plate layered with silica gel and then adjusted on the sampler of the instrument.

The Transmission electron microscope (TEM) images were taken on Hitachi (H-7500). The sample was dispersed in ethanol and one drop of the dispersion was placed on a 200 mesh carbon coated copper grid. Solvent was evaporated and images recorded at different magnifications.

The thermal properties of the nanocomposites were studied by using Differential scanning calorimeters DSC-6 of Shimadzu. For the analysis 5 mg of the sample was placed on an aluminium pan of 50 μm thickness, sealed and heated up to 100 °C. The specimens were cooled to room temperature and then scanned from 27 to 300 °C at a constant rate of 10 °C / min. Thermogravimetric Analysis (TGA, Shimadzu DTG-60H) was performed to determine the thermal stability of the samples. The measurements were performed under nitrogen atmosphere and the heating rate was 10 °C / min

Molecular weight and molecular weight distribution of the nanocomposites were determined by gel permeation chromatography (GPC, Perkin Elmer 200 Series with refractive index detector) using polystyrene as standard. Column used was mix PL gel 10^3 and THF (Tetrahydrofuran) with a flow rate of 1 mL/min was used as mobile phase.

^{13}C NMR spectra were recorded with Bruker-400 MHz NMR spectrometer at room temperature with $CDCl_3$ solvent. ^1H NMR spectra was recorded with Bruker Avance II 400 NMR spectrometer.

Photochemical degradation of methylene blue

10 ml of 10^{-5} M solution of methylene blue dye (MB) was taken in a 50 ml beaker. 50 mg of ZnO/PLLA nanocomposite (2 % ZnO) was added as photocatalyst and the solution stirred on a magnetic stirrer for 1 h in dark to disperse the catalyst. The solution was then exposed to UV light and the rate of degradation of MB was studied UV-Visible spectrophotometer. The kinetics of the reaction was studied by

measuring the absorption of solution at 665 nm at different time intervals.

Results and discussion

Among the various methods available for synthesis of metal oxide nanoparticles, we have chosen microwave technique [26] to synthesize the ZnO nanoparticle because; the technique is time saving in comparison to other hydro and solvothermal methods. Starting material used was Zinc acetate, which is nontoxic to human and is used as a food additive. Melt mixing of the polymer with nanoparticles is generally used to synthesize nanocomposites. However, it is generally not sufficient to bring about uniform dispersion of hydrophilic metaloxide nanoparticles into the polymer matrix and in most instances, surface modification of the nanoparticles becomes essential [17]. In contrast, in-situ polymerization [27] approaches allow direct and easy dispersion of nanoparticles into the polymer matrix with improved interfacial interaction. Bulk ZnO has been reported to catalyze the polymerization of L-lactide with high optical purity and conversion [28]. In the present work, we explored the usage of ZnO nanoparticles as catalyst as well as multifunctional filler for synthesizing PLLA/ZnO nanocomposite. A number PLLA/ZnO nanocomposites with varying concentration (0.5 to 10 %) of ZnO nanoparticles were synthesized to study various properties. Most of the properties were studied for ZnO concentration upto 2 % only. We have prepared polymer/ZnO with higher ZnO conc. (5 % and 10 %) in order to study some parameters in IR and XRD. We also observed that with increasing ZnO content composite becomes almost insoluble and mass determination was not possible. Hence further discussion of these was not done. Isolated samples at all concentrations of ZnO were found to be pristine white in colour.

FT-IR analysis was used to study the chemical structure of all the samples. Figure 1 shows FT-IR spectra of bare ZnO nanoparticles, PLLA/ZnO nanocomposites (2 %) and PLLA standard sample. In the case of ZnO nanoparticles, a strong absorption band observed between 480 and 420 cm^{-1} was attributed to the stretching modes of Zn-O [29]. The peaks at 1,581 and 1,412 cm^{-1} are due to O–C–O stretching of surface groups of ZnO. The broad absorption peak between 3,300 and 3,500 cm^{-1} can be attributed to the stretching vibrations of surface hydroxyl groups.

FT-IR spectrum of standard PLLA showed the most intense bands between 1,759 and 1,762 cm^{-1} corresponding to—C = O stretching vibration of carbonyl group from the repeated ester unit. The -C-O - stretching vibrations of ester in the main chain were observed at 1,200, 1,124 and 1,100 cm^{-1} Two significant peaks observed at 2,997 and 2,889 cm^{-1} were assigned to the asymmetrical and symmetrical—C–H stretching of the methyl group in the side chains. The corresponding bending vibrations of—CH_3 group were observed at 1,455 cm^{-1}. The band at 2,945 cm^{-1} was attributed to stretching of—CH group present in the main chain of PLLA and the symmetrical and asymmetrical bending vibration corresponding to this group appeared at 1,386–1,360 cm^{-1}. The small peak observed at 1,621–1,604 cm^{-1} in the FT-IR spectrum of PLLA/ZnO nanocomposite was attributed to the O═C═O stretching of the chain ending carboxylate groups.

FTIR bands characteristic of PLLA [30] were also observed in the spectrum of PLLA/ZnO nanocomposite. The band due to –C = O stretching appeared as the most intense

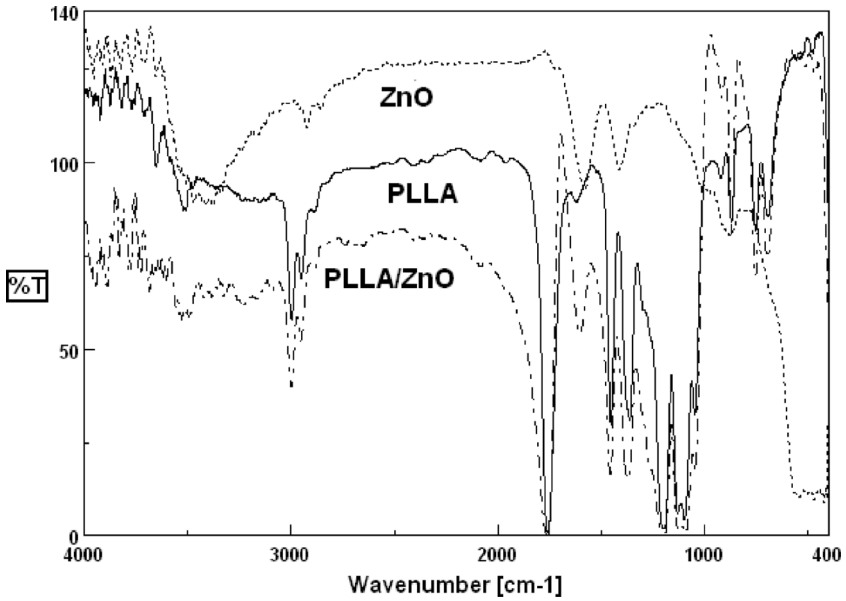

Fig. 1 FT-IR spectrum of ZnO, PLLA/ZnO nanocomposites (2 %) and PLLA (standard sample)

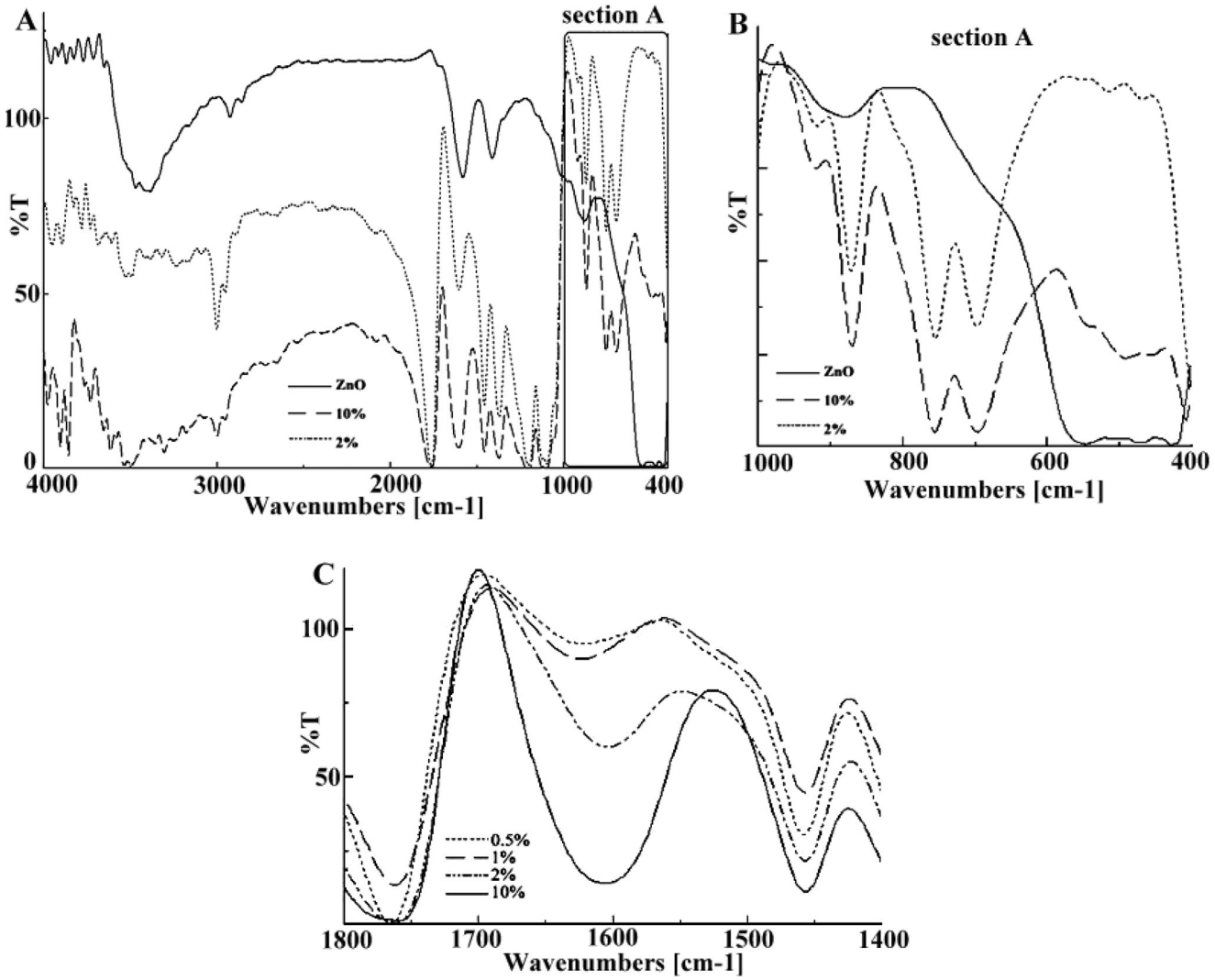

Fig 2 **a** The FTIR spectra of PLLA/ZnO nanocomposites (2 and 10 %) and ZnO nanoparticles (**b**) Magnified FTIR spectra of PLLA/ZnO nanocomposites (2 and 10 %) and ZnO nanoparticles (**c**) Magnified FTIR spectra of PLLA/ZnO nanocomposites

band at 1,758 cm^{-1}. No splitting of this band was observed as mentioned by some of the workers. The chain ending stretching of the chain ending carboxylate groups appeared slightly shifted at 1,621–1,604 cm^{-1} with enhanced intensity. Shift in the peak may be due to its proximity to the ZnO nanoparticles.

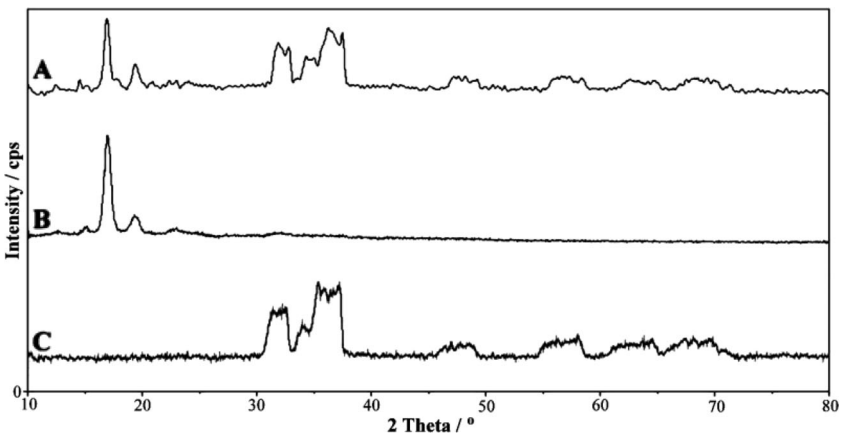

Fig. 3 Powder XRD stack view of (**a**) PLLA/ZnO nanocomposites (10 %), **b** PLLA/ZnO (2 %) (**c**) ZnO nanoparticles

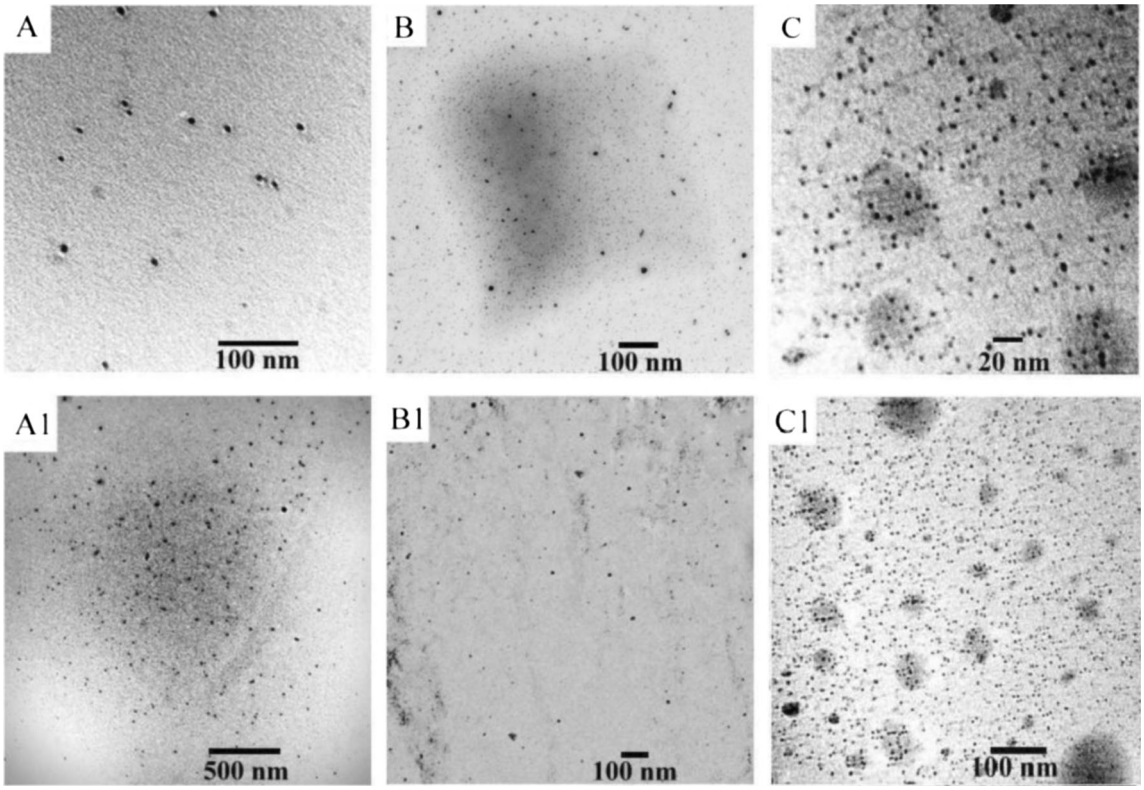

Fig. 4 TEM micrographs of 0.5 % (**a** and A1), 1 % (**b** and B1) and 2 % (**c** and C1) PLLA/ZnO nanocomposites

The intensity of this band increases with the increase in the concentration of ZnO nanoparticles in the PLLA/ZnO nanocomposite as shown in Fig. 2c. At low concentration of ZnO in the nanocomposite, its characteristic Zn-O stretching at 480–420 cm^{-1} was not observed in the FTIR spectrum. However, we prepared a sample with 10 % ZnO concentration and were able to observe this peak [Fig. 2a and b].

A comparison of powder XRD analysis of ZnO nanoparticle, PLLA and PLLA/ZnO (10 %) nanocomposites is shown in the Fig. 3. XRD of ZnO nanoparticles showed the characteristics peaks centered at 31.9, 36.26, 37.48, 47.63, 56.66, 69.33° 2θ values. A large broadening of the peaks indicated the nanosize of ZnO nanoparticles. The peaks were indexed to the hexagonally wurtzite structure of ZnO nanocrystal and were assigned to (1 0 0), (0 0 2), (1 0 1), (1 0 2), (1 1 0), (1 0 3), (1 1 2), (2 0 0) and (2 0 1) reflections in accordance with International Center for diffraction data, JCPDS No.36-1451. PLLA/ZnO nanocomposites (up to 2 % ZnO) showed peak at 2θ value 16.9 ° corresponding to PLLA only [31]. Peaks corresponding to ZnO were not observed. However, in a sample prepared with higher ZnO concentration (10 %), we could observe peaks corresponding to ZnO as well as PLLA. It is also evident that the crystalline peak of PLLA at 16.9 (2θ value) decreases with increasing content of ZnO.

TEM images (Fig. 4) of various PLLA/ZnO nanocomposites showed the morphology of the nanocomposites and the size of the nanoparticles. Water melon type morphology was observed in which ZnO nanoparticles of 2 to 4 nm dimension were dispersed in a continuous polymer phase. It could also be observed that even with the increase in the content of ZnO, no agglomeration of particles occurred. This may be due to the fact that polymerization started at the surface of ZnO nanoparticles and the growing polymer chains push the nanoparticles apart and don't allow them to agglomerate. SEM image (Fig. 5) for PLLA/ZnO nanocomposites (2 %) showed a continuous morphology for the nanocomposite.

Typical ^{1}H and ^{13}C spectra are shown in Fig. 6. ^{1}H NMR of the nanocomposite dispersed in $CDCl_3$ showed strong signals

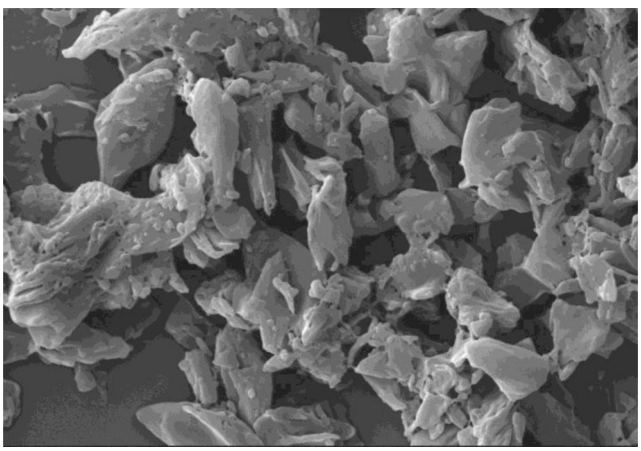

Fig. 5 SEM of the PLLA/ZnO nanocomposite (2 %)

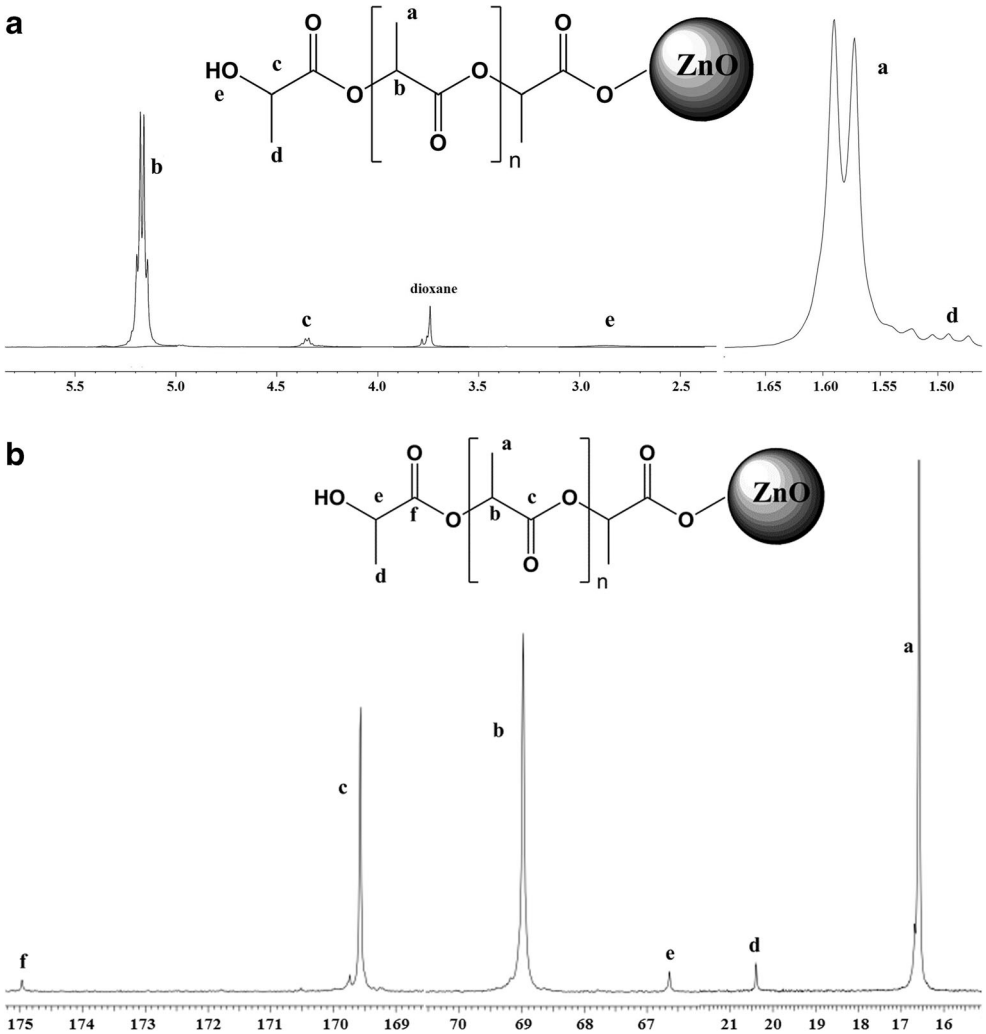

Fig. 6 **a** ^{1}H NMR spectrum of PLLA/ZnO nanocomposites (2 %): **b** ^{13}C NMR spectrum of PLLA/ZnO (2 %) nanocomposites

at 1.56 and 5.18 ppm corresponding to methyl and methine protons of the PLLA chain. Relatively weak quartet at 4.35 ppm was assigned to methine proton attached to the terminal hydroxyl group. Another weak peak at 1.35 ppm was assigned to the methyl group in the vicinity of terminal hydroxyl group. The broad peak in the range of 3.5–3.8 ppm attributed to hydroxyl end groups. Clear quartet at 5.18 also indicates the optical purity of poly (lactide). Thus, it can also

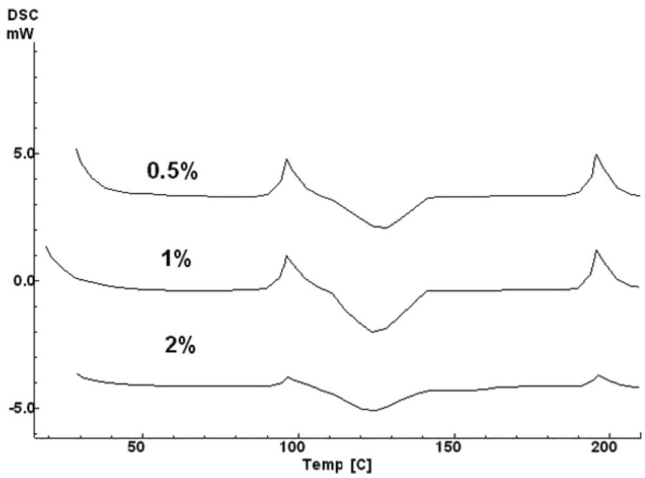

Fig. 7 The DSC thermogram (second run) of PLLA/ZnO nanocomposites (0.5, 1, 2 %)

Table 1 Thermal properties for PLLA/ZnO nanocomposites determined from DSC thermograms

Sr. No.	PLLA/ZnO	Tc (°C) ΔHc (J/g)	Tm (°C) ΔHm (J/g)	Td (°C)
1	0.5 %	96.27 28.98	128.42 −70.4	203
2	1 %	96.07 24.16	123.67 −65.10	242
3	2 %	96.55 12.94	124.79 −46.97	210

Tc temperature of crystallization, ΔHc enthalpy of crystallization, Tm melting temperature, Td Onset of decomposition

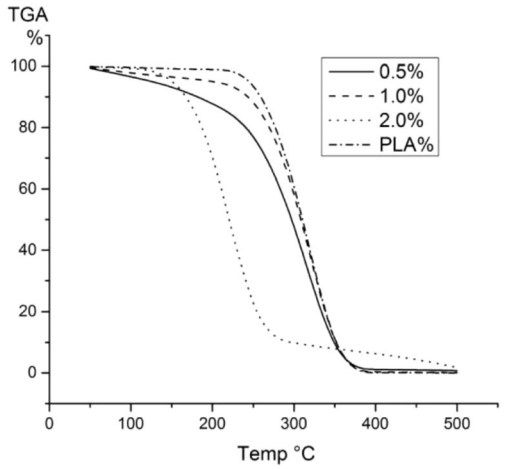

Fig. 8 TGA curves of PLLA/ZnO nanocomposites (0.5, 1, 2 %)

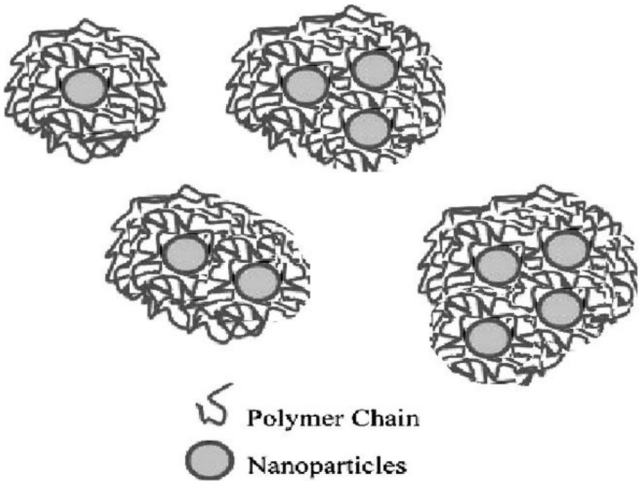

Fig. 9 Graphical representation of PLLA/ZnO nanocomposite structure

be concluded that no racemization occurred during the polymerization. ^{13}C NMR corroborated the results shown by ^{1}H NMR. Signals corresponding to methyl and methine protons of the repeating monomer were observed at 16.59 and 68.98 ppm respectively. The main chain carbonyl carbon showed a strong peak at 169.57 with only a small shoulder at 169.74 indicating a highly isotactic polymerization [30, 32]. The weak peaks at 66.63, 20.39 and 174.5 ppm were assigned to methine, methyl and carbonyl carbon of the hydroxyl end terminal. Carboxylic end groups and methyl and methine groups next to it could not be identified in either ^{1}H or ^{13}C NMR. This too points towards attachment of the carboxylate group to the ZnO surface.

Thermal properties of the nanocomposite were studied by DSC and TGA. Figure 7 presents the DSC thermal scans of various PLLA/ZnO nanocomposites. All PLLA/ZnO nanocomposites showed similar thermal traces. The glass transition temperature (Tg) is recognised as one of the most important parameter for the technological application of the polymers. Surprisingly, it was not observed at all in the DSC scan of PLLA/ZnO nanocomposite whereas, in the standard PLLA sample it appeared at 78.3 °C. Interfacial interactions and confinement of polymers can alter their Tg. Such observation has been also made by other researchers when polymer chains are confined i.e. between clay layers [33]. In the present case, this may be due to attachment of polymer chains by both the ends to the surface of nanoparticles, thus slowing segmental motion and material is frozen. DSC of the nanocomposite first run and second run (Fig. 7b) were also found to be different. First run showed two melting peaks at 127.6 and 162.0 °C. This changed to only one melting temperature observed at 144.6 °C in the second run. An increase in enthalpy of crystallization (96.2 °C) was observed in the in the second run. DSC of the nanocomposite showed two crystallization peaks (Tc) and the melting process (Tm). Observed thermal data from second DSC run are compiled in Table 1. It was found that the peak area under the melting point curve decreased with the increase in the content of ZnO nanoparticles. This result also indicated that the crystallinity of PLLA/ZnO nanocomposites decreased as the content of ZnO nanoparticles increased and is consistent with the XRD data.

The thermal stability of the nanocomposite was studied by thermogravimetric analysis under nitrogen. The weight loss due to formation of volatile products after degradation is monitored as a function of temperature. Figure 8 shows the TGA thermograms of pure PLLA and PLLA/ZnO nanocomposites at various concentrations of ZnO. Polylactic acid degrades by chain unzipping mechanism and a slow initial degradation is followed by a fast weight loss without any char

Table 2 Average molecular weight of PLLA/ZnO nanocomposites (0.5, 1 and 2 %)

Sample	Mw	Mn	PDI
0.5 %	1,747	1,229	1.42
1 %	1,908	1,324	1.44
2 %	3,784	1,992	1.89

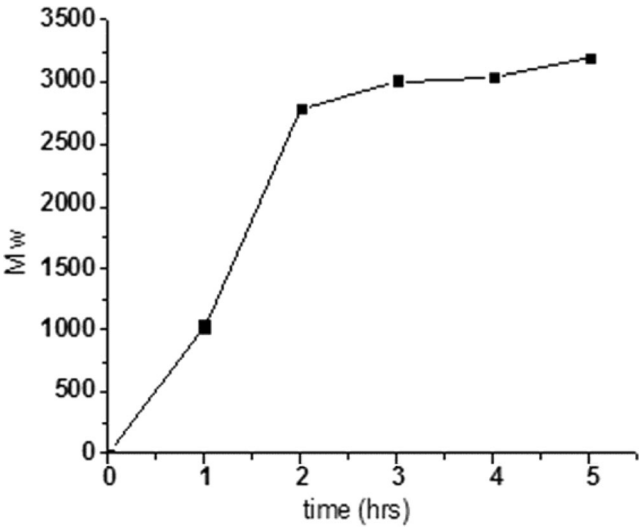

Fig. 10 Kinetics of polymerization

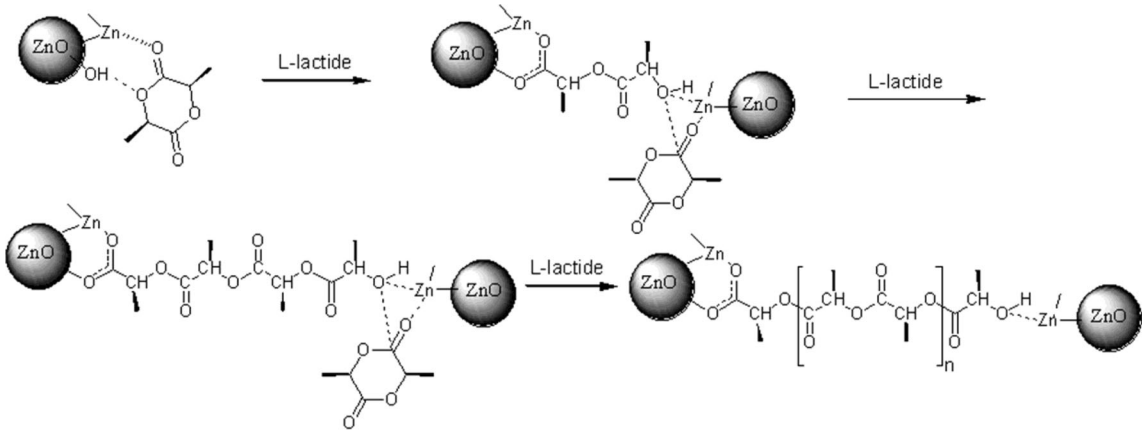

Fig. 11 Proposed mechanism and structure of the PLLA/ZnO nanocomposite

formation. The slow initial weight loss is attributed to presence of moisture or unreacted monomers and fast weight loss to unzipping of polymer chain. Similar patterns were observed in nanocomposites with 0.5 and 1 % ZnO content. However, in PLA/ZnO (2 %) a distinct change was observed. It showed a third region of slow degradation between 250 and 500 °C and was attributed to the polymer fraction closely association with the ZnO nanoparticles [30]. Final residue at 500 °C was 1.74 %. At low ZnO concentration degradation process was very broad. The degradation process became sharper with the increase in ZnO %. Murario et al. has reported that ZnO catalyzes unzipping of polylactide [17]. This may be the reason for fast degradation rate of nanocomposite at ZnO concentration of 2 %. Overall, a decrease in the melting point and crystallinity of PLLA was observed with increase in ZnO content.

GPC analysis of PLLA/ZnO (0.5, 1, 2 wt.%) nanocomposites was carried out by dissolving the nanocomposites in THF. PLLA/ZnO naocomposites did not dissolve completely in THF solvent and attempts to completely separate PLLA from ZnO by HCl extraction failed. Nanocomposites are only partialiy soluble in THF. So, these are molecular weights of only soluble fraction. Actual molecular weights of the prepared polymers might be higher. The results of GPC analysis for THF soluble fraction are shown in Table 2. It can be seen that the molecular weight of the nanocomposites keeps on increasing with increasing amount of ZnO nanoparticles. This seems unusual as the length of polymer chain and hence, size should decrease with the increase in catalyst concentration. The results can be explained if it is concluded that nanoparticles are strongly attached to the polymer and with the increase in ZnO concentration the hydrodynamic volume of the polymer increases as shown in Fig. 9. However, these results could not predict the true length of the polymer chain as PLLA is strongly attached to ZnO. Also the material was not completely dispersed in THF. The kinetics of polymerization at the monomer/catalyst ratio of 50/1 at 160 °C was also studied by GPC. During polymerization samples were withdrawn at different time intervals, dispersed in THF and Mw determined by GPC. A plot of Mw verses time is shown in Fig. 10.

On the basis of spectral evidence and properties, we propose above mechanism (Fig. 11) for the polymerization. Absence of racemization indicated that ring opening polymerization occured through coordination-insertion mechanism [34]. PLLA chains are probably strongly attached to ZnO surface through carboxylate group as well as H-bonding. Hydroxyl groups present on the surface of one ZnO

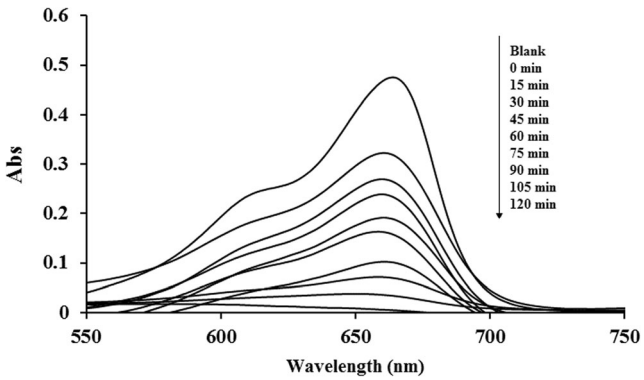

Fig. 12 UV-Visible absorbance of MB solution at 15 min interval

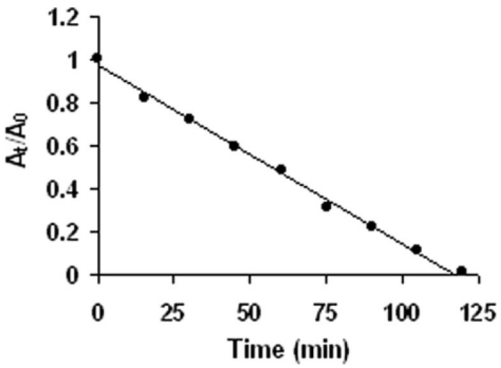

Fig. 13 Plot of MB absorbance (At/A0) at 665 nm verses time

nanoparticle act as initiator and Zn atoms on the suface of other nanoparticle provide the site for co-ordination. Thus polymer chain grew confined between the two nanoparticle. As polymerization can start from more than one point on the nanoparticle surface a water melon morphology, in which a large number of nanoparticles are embedded in the polymer matrix, is predicted for the nanocomposite.

Photocatalytic degradation of Methylene blue

ZnO nanoparticles are known to show photocatalytic properties that include degradation of dyes, phenols, formaldehyde etc. The most common dye used for the quantification of photocatalytic activity is methylene blue. The latter has a blue colour in oxidising environment [35]. During photocatalysis, the dye undergoes decomposition and turns colorless. The change in colour can be quantified spectrophtometrically by measuring the absorption of dye at 645 nm. We used this dye to study the photo-degradation property of the nanocomposite. It was observd that when the nanocomposite was stirred with the dye solution in dark, it absorbed dye and turned blue. The colour disappeared only after the solution was exposed to UV radiation. Change in concentration of MB on exposure to UV radiation was monitored at different time intervals as shown in Fig. 12. A ratio of absorbence at time t (A_t) to initial absorbence (A_0) verses time showed a straight line indicating a zero order reaction (Fig. 13). The photochemical degradation of dyes generally follows first order kinetics according to Eqs. 1 and 2 (Fig. 13).

$$-dC_{MB}/dt = kC_{MB} \quad (1)$$

Where, C_{MB} is the concentration of dye. In the present case there is excess of dye on the surface of catalyst due to absorption of dye by the PLLA. So the degradation becomes independent of dye concentration and hence Eq. 1 becomes.

$$-dC_{MB}/dt = k \quad (2)$$

Thereafter, effect of various factors like pH, presence of H_2O_2, amount of catalyst etc. on the dye degradation was also studied. Addition of hydrogen peroxide does not affect the rate of reaction. The reason could be the hydrogen peroxide attacks the surface of polymer under UV irradiation and does not affect the rate of reaction [36].

Effect of pH on the rate of dye degradation was studied by changing the pH of methylene blue solution. The degradation of methylene blue solution containing PLLA/ZnO nanocomposites was studies at pH 4, 6, 8 and 12. A graph showing fraction of MB degraded in 40 min at different pH is shown in the figure. There is increase in rate of degradation both at high as well as low pH. This can be due to the fact that formation of reactive

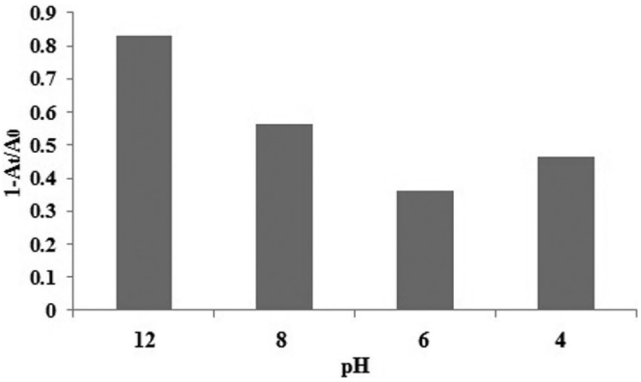

Fig. 14 Effect of pH on the rate of MB degradation

intermediates increases i.e. hydroxyl radicals significantly at low and high pH or it may be due to change in absorption of methylene blue by PLLA with pH.

$$ZnO + hv \rightarrow ZnO^{\cdot}$$
$$ZnO^{\cdot} + H_2O \rightarrow ZnO^{\cdot} + H^{+} + {}^{\cdot}OH$$
$${}^{\cdot}OH + Dye \rightarrow Intermediates \rightarrow CO_2 + H_2O$$

Effect of catalyst concentration was studied by changing the amount of nanocomposite while keeping the dye concentration constant. It was observed that there is increase in the rate of degradation with the increase in catalyst concentration. Degradation of dye at catalyst concentration of 50, 100 and 150 mg was carried out and results are shown in Fig. 15.

Conclusions

We have successfully synthesized PLLA/ZnO nanocomposites by ring opening polymerization of L-lactide monomer on the surface of ZnO nanoparticle. ZnO itself acted as catalyst and no additional catalyst was used. The method used was an environmentally benign process. The nanocomposites were characterized by FT-IR, DSC, TGA, XRD, TEM, GPC, ^{13}C and ^{1}H NMR. TEM results showed that the size of the nanoparticles ranged from 2 to 10 nm. In comparison to other

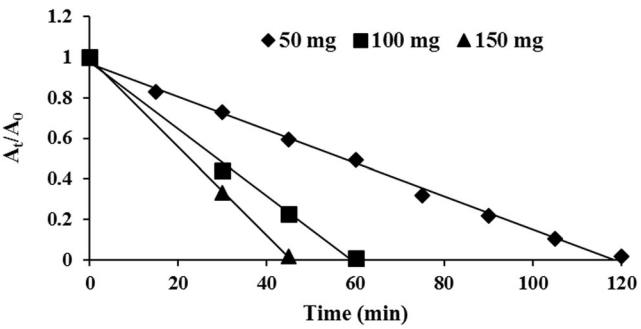

Fig. 15 Effect of nanocomposite concentration on the rate of MB degradation

techniques used for the preparation of PLLA/ZnO nanocomposites, this method showed better dispersion of ZnO nanoparticles in the PLLA matrix. The nanocomposite combined the photocatalytic properties of ZnO with absorbing properties of PLLA and efficiently degraded methylene blue.

Acknowledgments We greatly acknowledge Saurashtra University for ^{13}C NMR and TGA, SICART for GPC and SAIF, Chandigarh for ^{1}H NMR and TEM. One of the authors is grateful to University Grants commission (UGC), New Delhi for MANF to carry out this work.

References

1. Ikada Y, Tsuji H (2000) Biodegradable polyesters for medical and ecological applications. Macromol Rapid Commun 21:117
2. Tsuji H, Ikada Y (1998) Blends of aliphatic polyesters. II. Hydrolysis of solution-cast blends from poly (L-lactide) and poly (E-caprolactone) in phosphate buffer solution. J Appl Polym Sci 67:405
3. Urayama H, Kanamori T, Kimura Y (2002) Properties and biodegradability of polymer blends of poly (L-lactide) with different optical purity of the lactate units. Macromol Mater Eng 287:116
4. Jain RA (2000) The manufacturing techniques of various drug loaded biodegradable poly (lactide-co-glycolide) (PLGA) devices. Biomaterials 21:2475
5. Mikos AG, Lyman MD, Freed LE, Langer R (1994) Wetting of poly (L-lactic acid) and poly (DL-lactic-co-glycolic acid) foams for tissue culture. Biomaterials 15:55
6. Suzuki S, Ikada Y (2010) Aurus R, Lim LT, Selke SEM, Tsuji H (eds) poly(lactic acid) synthesis, structure, properties, processing and application. John Wiley and Sons Ltd. USA
7. Kamath KR, Park K (1993) Biodegradable hydrogels in drug delivery. Adv Drug Deliv Rev 11:59
8. Edlund U, Albertsson AC (2002) Degradable polymer microspheres for controlled drug delivery. Adv Polym Sci 157:67
9. Perego G, Cella GD, Bastioli C (1996) Effect of molecular weight and crystallinity on poly (lactic acid) mechanical properties. J Appl Polym Sci 195:1649
10. Sinclair RG (1996) The case of poly (lactic acid) as a commodity packaging plastic. J Macromol Sci Pure Appl Chem 33:585
11. Ray SS, Bousmina M (2006) In: Mai YW, Yu ZZ (eds) Polymer nanocomposites, wood head publishing Ltd. Cambidge England.
12. Jamshidian M, Tehrany EA, Imran M, Jacquot M, Desobry S (2010) Poly-Lactic Acid: production, applications, nanocomposites, and release studies. Compr Rev Food Sci F 9:552–571
13. Ray SS (2012) Polylactide-based Bionanocomposites. A promising class of hybrid materials. Acc Chem Res 45(10):1710–1720
14. Hiroi R, Ray SS, Okamoto M, Shiroi T (2004) Organically modified layered titanate: a new nanofiller to improve the performance of biodegradable polylactide. Macromol. Rapid Commun 25:1359–64
15. Nakayama N, Hayashi T (2007) Preparation and charecterization of poly(L-lactic acid/ TiO2 nanoparticle nanocomposite films with high transparency and efficient photodegradability. Polym Degrad Stab 92:1255–1264
16. Li Y, Sun XS (2010) Preparation and characterization of polymer-inorganic nanocomposites by in situ melt polycondensation of L-lactic acid and surface-hydroxylated MgO. Biomacromol 11:1847–1855
17. Murariu M, Doumbia A, Bonnaud L, Dechief AL, Paint Y, Ferreira M, Campagne C, Devaux E, Dubois P (2011) High-performance Polylactide/ZnO nanocomposites designed for films and fibers with special end-use properties. Biomacromol 12:1762–71
18. Hongjuan Z, Zhiwei Z, Yalong L, Xiaofeng Z, Xi K (2012) Preparation of PLA/nano-ZnO composites. Adv Mater Res 476:1901
19. Dang L, Fan S, Nan ZC (2003) Dielectric properties and morphologies of composites filled with whisker and nanosized zinc oxide. Mater Res Bull 38:499–50
20. Li YQ, Fu SY, Mai YW (2006) Preparation and characterization of transparent ZnO/epoxy nanocomposites with high-UV shielding efficiency. Polymer 47:2127–2132
21. Usui H, Shimizu Y, Sasaki T, Koshizaki N (2004) Photoluminescence of ZnO nanopar- ticles prepared by laser ablation in different surfactant solutions. J Phys Chem B 109:120–124
22. Li Y, Li G, Yin Q (2006) Preparation of ZnO varistors by solution nano-coating tech- nique. Mater Sci Eng B 130:264–268
23. Baruwati B, Kumar DK, Manorama SV (2006) Hydrothermal synthesis of highly crystalline ZnO nanoparticles: a competitive sensor for LPG and EtOH. Sens Actuators B 119:676–682
24. Yi GC, Wang C, Park WI (2005) ZnO nanorods: synthesis, characterization and applications. Semicond Sci Technol 20: S22–S34
25. Therias S, Larché J-F, Bussière P, Gardette J-L, Murariu M, Dubois P (2012) Photochemical behavior of polylactide/ZnO nanocomposite films. Biomacromol 13:3283–3291
26. Bilecka I, Elser P, Niederberger M (2009) Kinetic and thermodynamic aspects in the microwave assisted synthesis of ZnO nanoparticles in benzyl alcohol. ACS Nano 3:467–477
27. Althues H, Simon P, Philipp F, Kaskel S (2006) Integration of zinc oxide nanoparticles into transparent poly(butanediolmonoacrylate) via photopolymerization. J Nanosci Nanotechnol 6:409–413
28. Kricheldor HR, Serra A (1985) Polylactones 6. Influence of various metal salts on the optical purity of poly(L-Lactide). Polym Bull 14: 497–502
29. Li F, Xintang H, Yin J, Luoyuan L, Zhen L (2009) Synthesis and characterization of ZnO/SiO_2 core/shell nanocomposites and hollow SiO_2 nanostructures. Mater Res Bull 44:437
30. Garllota D (2002) A literature review of poly (Lactic Acid). J Polym Environ 9:63–84
31. Pan P, Inoue Y (2009) Polymorphism and isomorphism in biodegradable polyesters. Prog Polym Sci 34:605–640
32. Bero M, Kasperczyk J, Jedlinski Z (1990) Coordination polymerization of lactides, 1. Structure determination of obtained polymers. Die Makromolekulare Chemie 191:2287–2296
33. Caseri WR (2006) Nanocomposites of polymers and inorganic particles: preparation, structure and properties. Mater Sci Tech 22:807–817
34. Gupta AP, Kumar V (2007) New emerging trends in synthetic biodegradable polymers-Polylactide: a critique. Eur Polym J 43:4053–4074
35. Jang YJ, Simer C, Ohm T (2006) Comparison of zinc oxide nanoparticles and its nano-crystalline particles on the photocatalytic degradation of methylene blue. Mat Res Bull 41:67–77
36. Zuwei M, Changyou G, Jun Y, Jian J, Yihong G, Jiacong S (2002) Surface modification of poly L-lactide by photografting of hydrophilic polymers towards improving its hydrophilicity. J App Polym Sci 85:2163–2171